remote sensing

MDPI

Technical Note

Asymmetric Distribution of Plasma Blobs During High Solar Activity in the Low- to Middle-Latitude Ionosphere

Zhuo Huang [1], Jia Zhu [2], Weihua Luo [1,3,*], Zhengping Zhu [1,3,4], Guodong Jia [2] and Shanshan Chang [1,3]

[1] College of Electronic and Information Engineering, South-Central Minzu University, Wuhan 430074, China; 2022110185@mail.scuec.edu.cn (Z.H.); 3082907@mail.scuec.edu.cn (Z.Z.); 2014064@mail.scuec.edu.cn (S.C.)
[2] School of Electronic Information, Wuhan University, Wuhan 430072, China; zhujia@whu.edu.cn (J.Z.); 2024182120085@whu.edu.cn (G.J.)
[3] Key Laboratory of Electronic Information Engineering (State Ethnic Affairs Commission), South-Central Minzu University, Wuhan 430074, China
[4] Hubei Engineering Research Center of Intelligent Internet of Things Technology, South-Central Minzu University, Wuhan 430074, China
* Correspondence: whluo@mail.scuec.edu.cn

Abstract: Using the data from the first satellite of the Republic of China (ROCSAT-1) obtained during high-solar-activity periods (2000–2003), the distributions of plasma density enhancement (plasma blobs) with local time, season and longitude were investigated. Some new features of plasma blobs can be concluded: (a) The distribution of plasma blobs shows remarkable seasonal and interhemispheric asymmetries, with the higher occurrence in June solstice months and in the winter hemisphere. (b) The occurrence of plasma blobs displays longitude dependence, more in the −180~−90°E, −60~0°E and 90~180°E longitude regions. (c) The seasonal and interhemispheric asymmetries of plasma blobs also depend on the longitude. Meridional wind plays an important role in the formation and evolution of low-latitude plasma blobs. Inclination and declination may control the longitudinal distribution of plasma blobs.

Keywords: low-latitude ionosphere; plasma blob; asymmetry; meridional wind

Academic Editor: Yunbin Yuan

Received: 27 November 2024
Revised: 26 December 2024
Accepted: 26 December 2024
Published: 28 December 2024

Citation: Huang, Z.; Zhu, J.; Luo, W.; Zhu, Z.; Jia, G.; Chang, S. Asymmetric Distribution of Plasma Blobs During High Solar Activity in the Low- to Middle-Latitude Ionosphere. *Remote Sens.* **2025**, *17*, 82. https://doi.org/10.3390/rs17010082

1. Introduction

Plasma density irregularities, which usually occur during nighttime periods, have two categories in the equatorial and low-latitude ionospheres. One manifests the depletion of plasma density about 2~3 orders according to the background density, also referred to as equatorial plasma bubbles (EPBs) [1]. The other displays density enhancement, or "plasma blobs" [2]. These plasma irregularities can affect the propagation of electromagnetic waves and degrade communication and navigation systems, causing ionospheric scintillation.

The climatology of EPBs has been extensively studied and reported by various measurements, such as ground-based ionosonde, GNSS, radar, satellite in situ and airglow observations. And the mechanism leading to the initiation and occurrence of EPBs is attributed to the generalized Rayleigh–Taylor (R-T) instability [1].

In contrast, there are fewer studies on the characteristics and mechanism of the plasma blobs, after the first report by Watanabe and Oya [2]. Some common features of plasma blobs from multiple measurements can be concluded as follows [3]: (a) Plasma blobs prefer to occur around 10~20° off the dip equator [4–6]. (b) The occurrence of blobs is higher during the June/December solstices than in the March/September equinoxes [3,5,6]. (c) The maximum occurrence rate is around local midnight [6,7]. Based on case studies, some different mechanisms accounting for the appearance of plasma blobs are proposed. Le

et al. [8] suggested, for the first time, that the occurrence of plasma blobs can be related to plasma bubbles due to the polarized electric field [9], and neutral wind would also play a vital role in the initiation of plasma blobs [10–12]. Some reports provided evidence that plasma bubbles can evolve into blobs from multiple measurements [13,14]. Medium-scale traveling ionospheric disturbances (MSTIDs) are another candidate for the formation of plasma blobs, due to the similar characteristics between MSTIDs and blobs [15–17]. Moreover, blobs are detected in the absence of bubbles and in the presence of MSTIDs in middle latitudes [15,17–19].

However, there are still some questions to be raised for the occurrence/mechanism of plasma blobs: (1) When or where would the blobs prefer to occur? (2) Is the blob locally generated from the equatorial region or higher-latitude region? (3) Can the formation of plasma blobs be related to the initiation and evolution of plasma bubbles? (4) What is the major mechanism for the blobs? Is it associated with plasma instability or other factors, e.g., MSTIDs?

Accurate knowledge of the statistical characteristics of plasma blobs and of the relationship between plasma bubbles and blobs, which we do not have yet, is crucial to study the mechanism leading to the occurrence of plasma blobs. Using data from the first satellite of the Republic of China (ROCSAT-1) during quiet periods in high solar activity (2000–2003), a new method was applied to depict the characteristics of plasma blobs, by identifying plasma blobs and their longitude range, and the distributions of plasma blobs depending on local time, season and longitude in the two hemispheres are reported. The factors causing the occurrence and variation of blobs are also discussed.

2. Data and Method

The ROCSAT-1 satellite was launched on March 1999 to a circular orbit at 600 km, with a 35° inclination and a period of 97 min, ending in June 2004. The onboard ionospheric and plasma electrodynamics instrument (IPEI) operates at 100% duty cycle to take continuous detections of ion density and composition covering all the longitude sectors in the low- to middle-latitude ionosphere [19], and inclined ROCSAT-1 orbit can reach to dip latitude of above ±35° in some longitude regions [7], which provides a good opportunity to study the longitudinal and seasonal variations of ion irregularities in the topside ionosphere.

The same method as that of Su et al. [20] and Su et al. [7] was used to identify the plasma irregularities. We use a 10-s boxcar window function in a segment of ROCSAT-1 data in time series to detect if the density variation fits the selection criterion. For each 10-s data segment, the density fluctuation is calculated using Equation (1)

$$\sigma = \frac{\left[\frac{1}{10}\sum_{i=1}^{10}(logn_i - logn_{oi})^2\right]^{1/2}}{\frac{1}{10}\sum_{i=1}^{10} logn_{oi}} \quad (1)$$

where n_i is the measured ion density and n_{oi} is the linearly fitted value at the ith data point.

At $\sigma > 0.3\%$, it is thought that a plasma irregularity has been found. To determine whether the irregularity belongs to a plasma bubble or plasma blob, we calculate the discrete numerical integration of raw and fitted ion density data within the moving window, with the time interval of 10 s. The discrepancy (Δcum) between raw density and fitted density is computed, and the total of all Δcum values is calculated as Δsum. The irregularity is identified as a plasma blob when the Δsum exceeds the threshold of 0.15×10^{-3} cm^{-3}. The longitude ranges (Δlon) in degree of plasma blobs are identified by use of the fitted ion density and recorded, represented by the spatial interval of satellite track in longitudes. Figure 1 shows an example of plasma blobs with different longitude ranges recorded by

ROCSAT-1 on 8 January 2001. The red dashed line in the figure represents the fitted density. The longitude ranges (Δlon) of plasma blobs are also marked. These four plasma blobs in Figure 1 showed different density fluctuations. For case a, the plasma density increased from 3.981 $\times$ 10^5 cm^{-3} to 5.011 $\times$ 10^5 cm^{-3}; density enhancement was about 25.9% relative to the background. The blob (case d) had more significant density fluctuations, with an enhancement about 336.5% relative to the background.

Typically, the longitude range of plasma blobs is about 1~3°, and large blobs can reach around 6°, which is similar to the case with plasma bubbles [21].

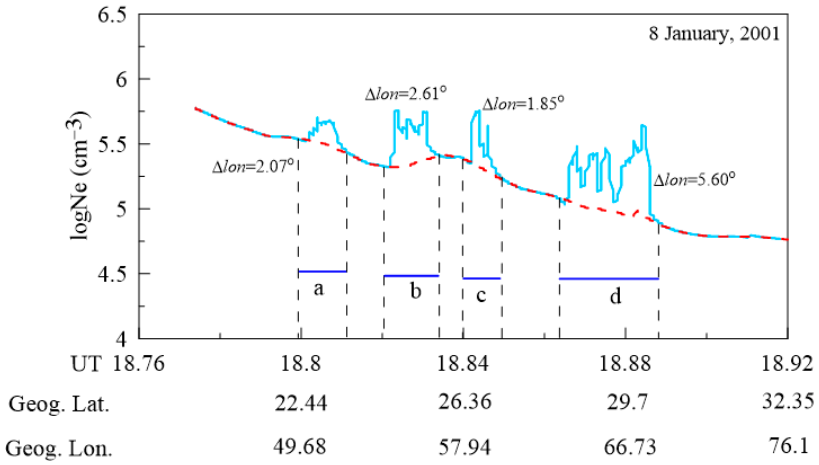

Figure 1. Examples of four plasma blobs (a, b, c, d) recorded by ROCSAT-1 on 8 January 2001. Longitude ranges of plasma blobs (Δlon) are marked. The red dashed line represents the fitted electron density.

3. Results

Figure 2 displays the seasonal and latitudinal–longitudinal distribution of medium longitude ranges of nighttime plasma blobs (0.45° < Δlon < 9.00°) from 1800 local time (LT) to 0600 LT in the low to middle ionosphere.

Plasma blobs prefer to occur in the low- to middle-latitude region around ±20°N, in the June and December solstices. The distribution of plasma blobs also depends on the longitude, with the higher occurrences in the −180~−90°E, −60~0°E and 90~180°E longitude regions.

The seasonal and latitudinal–longitudinal distributions of plasma blobs shown in Figure 2 are consistent with the previous reports by Su et al. [7] and Choi et al. [3]. We also notice that the longitude ranges of most plasma blobs are less than 6°, which is comparable to that of plasma bubbles, with a extent of 0–6° [21,22]. The blobs with longitude ranges larger than 6° are few. Hence, we can study the characteristics of plasma blobs based on the distributions of blobs at medium longitude ranges (0.45–6°).

Figure 3 presents the longitudinal and seasonal distribution of plasma blobs at medium longitude ranges (0.45° < Δlon < 6°) in the magnetic northern hemisphere (0~35°N) and southern hemisphere (−35~0°N) during 2000–2003.

From Figure 3, we can notice that the occurrence of plasma blobs shows remarkable seasonal and hemispheric asymmetries. In general, plasma blobs occur mainly in two solstice months, and the occurrence is higher in the June solstice (May–August) than in the December solstice (November–February) in most of longitude sectors in both the northern and southern hemispheres. For example, in the 0~60°E sector, in the both northern and southern hemispheres, plasma blobs mainly occur mainly in the June solstice and rarely in the December solstice or other months. Furthermore, the occurrence of plasma blobs in the southern hemisphere is higher than in the northern hemisphere. For example, in the

120~180°E sector, in the June solstice, plasma blobs occur more frequently in the southern hemisphere than in the northern hemisphere.

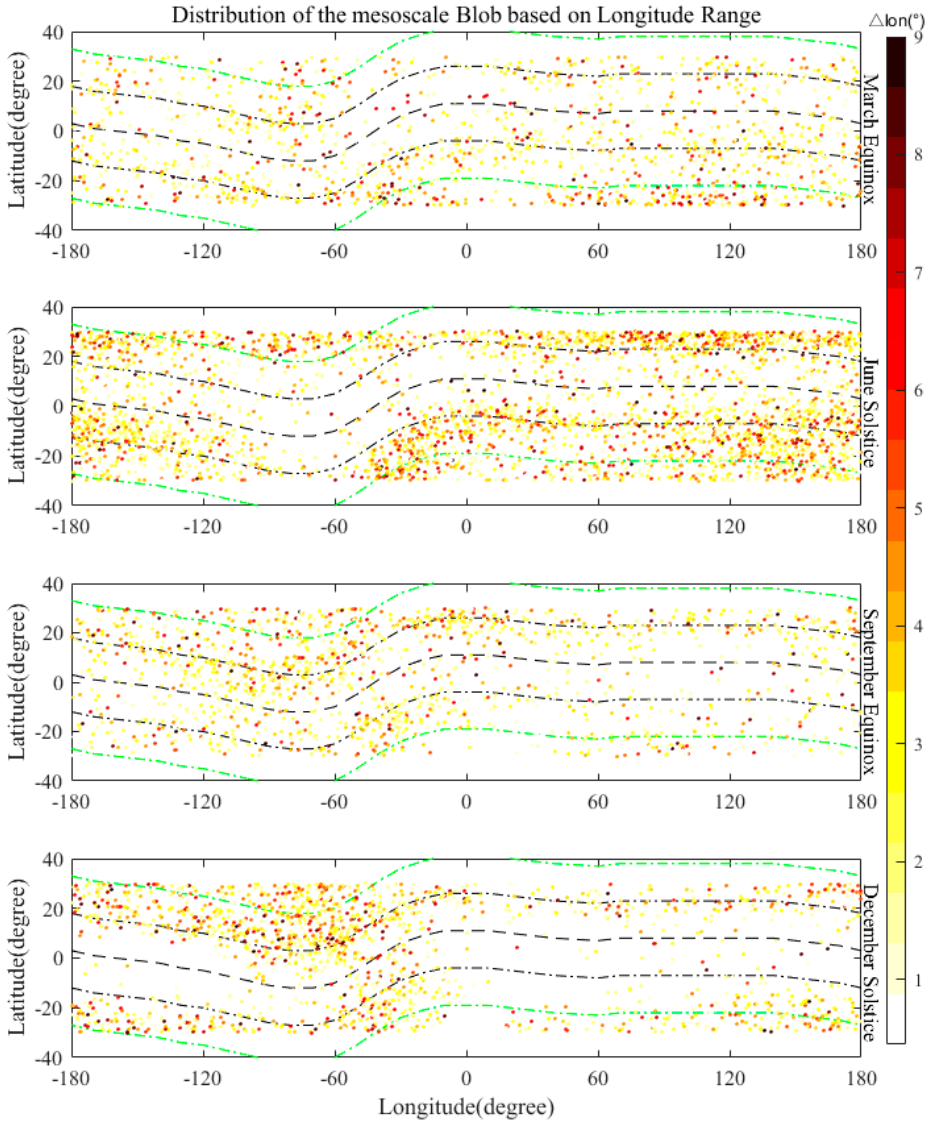

Figure 2. The latitudinal and longitudinal distribution of medium-longitude ranges of nighttime plasma blobs ($0.45° < \Delta lon < 9.00°$) in the low to middle ionosphere during 1800 LT–0600 LT in the March equinox, June solstice, September equinox and December solstice. The black dashed line represents the dip equator, and the black dot-dashed lines represent the dip latitude of ±15°; the green dot-dashed lines represent the dip latitude of ±30°.

Moreover, the seasonal and hemispheric asymmetry of plasma blob distribution also depends on the longitude. In the June solstice, plasma blobs occur in all the longitude sectors, except in the −90~−60°E sector in the southern hemisphere. Plasma blobs occur more frequently in the northern hemisphere in some longitudinal sectors, while the occurrence is higher in the southern hemisphere in other longitudinal sectors.

For instance, in the −90~−60°E sector, marked by the magenta rectangle in Figure 3, the highest occurrence is in the December solstice (winter hemisphere), and blobs occur mostly in the northern hemisphere and rarely in southern hemisphere. In the −150~−90°E sector, in the December solstice (winter hemisphere), plasma blobs occur mostly in the northern hemisphere. In the −45~0°E sector, marked by the blue oval, plasma blobs occur mostly in the southern hemisphere during the December solstice months (summer hemisphere) and rarely in the northern hemisphere, but the occurrence in the southern

hemisphere during the June solstice months (winter hemisphere) is higher than during the December solstice months.

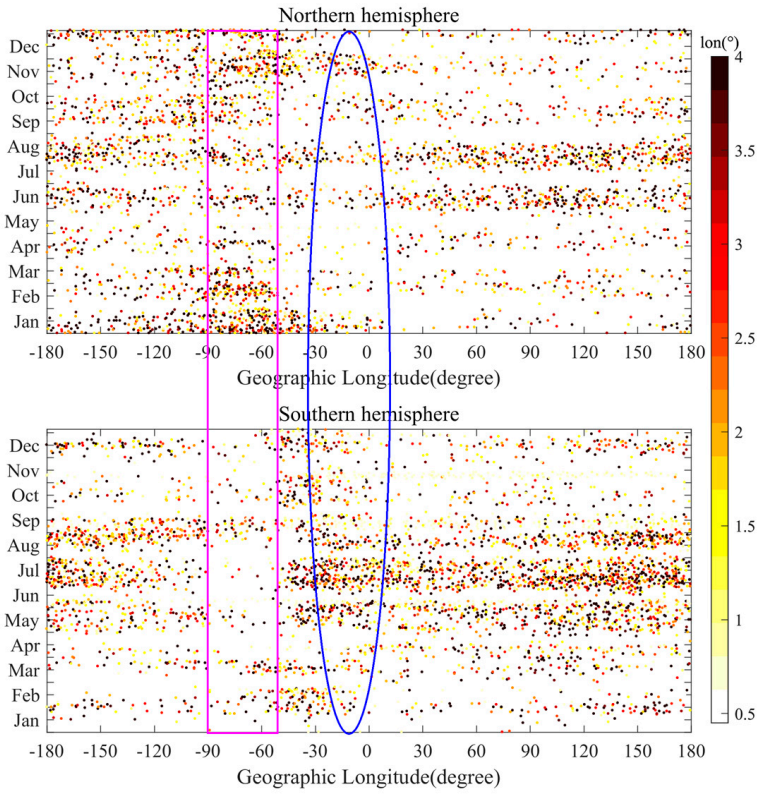

Figure 3. Longitudinal and seasonal distribution of plasma blobs with different longitude ranges in magnetic northern (**top**) and southern (**bottom**) hemispheres during 2000–2003.

Thus, we can offer the conclusion that plasma blobs prefer to occur in the June solstice and in the winter hemisphere in most of longitudinal sectors, which is consistent with the results from CNOFS during August 2008–April 2010 [3] and 52 cases from CHAMP during August 2002–July 2004 [6]. The results also indicate that the interhemispheric asymmetry of plasma blobs can be revealed, and it is viable to study the characteristics of plasma blobs from the distribution of blobs with different longitude ranges.

In Figure 4, to emphasize the interhemispheric asymmetry of plasma blob distribution between the summer and winter hemispheres, we display the distribution of plasma blobs depending on the longitude and local time in the summer hemisphere (May–August in the northern hemisphere and November–February in the southern hemisphere) and winter hemisphere (November–February in the northern hemisphere and May–August in the southern hemisphere), respectively. The red lines in the figure represent the local midnight.

As shown in Figure 4, the occurrence of plasma blobs shows the significant summer–winter hemispheric asymmetry: plasma blobs prefer to occur in the winter hemisphere in all longitudinal sectors. For example, in the −120~−60°E sector, plasma blobs occur rarely in the summer hemisphere.

In addition, the distribution of plasma blobs also displays longitudinal dependence. In the 120~180°E and −60~−30°E longitude sectors, plasma blobs occur more frequently than in other longitude regions. Moreover, in the summer and winter hemispheres, plasma blobs mainly occur after 2000 LT, and most blobs occur during 2200–0200 LT. In the early evening after sunset, the longitude ranges of blobs are usually small, such as around the −60~−30°E region.

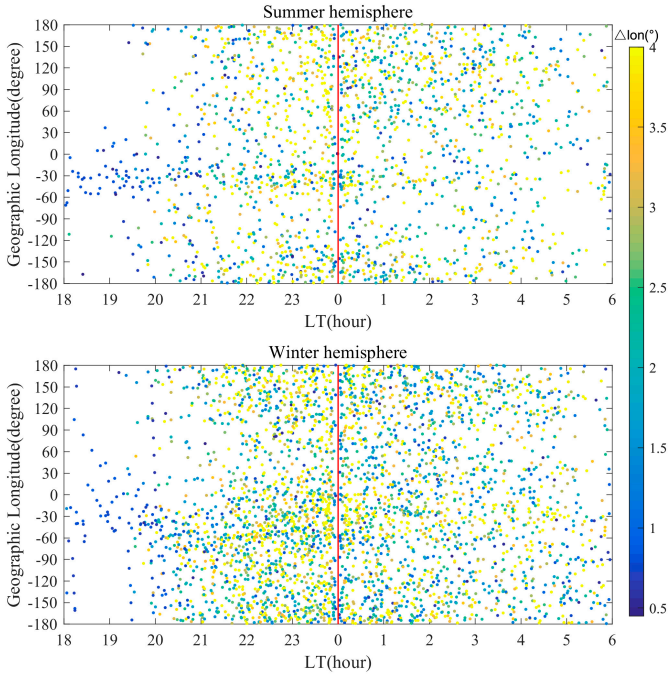

Figure 4. Longitude–local time variations of plasma blobs with different longitude ranges in the summer hemisphere (**top**) and winter hemisphere (**bottom**) during 2000–2003. The red lines represent midnight.

Furthermore, we divide the blobs into two parts: one is located in equatorial and low-latitude regions (−20°~20°N), and the other occurs in low- to middle-latitude regions (−35~−20°N and 20~35°N). Similar to Figure 4, Figure 5 and Figure 6 display the distribution of plasma blobs depending on the longitude and local time in the summer hemisphere and winter hemisphere in equatorial and low-latitude and low- to middle-latitude regions, respectively.

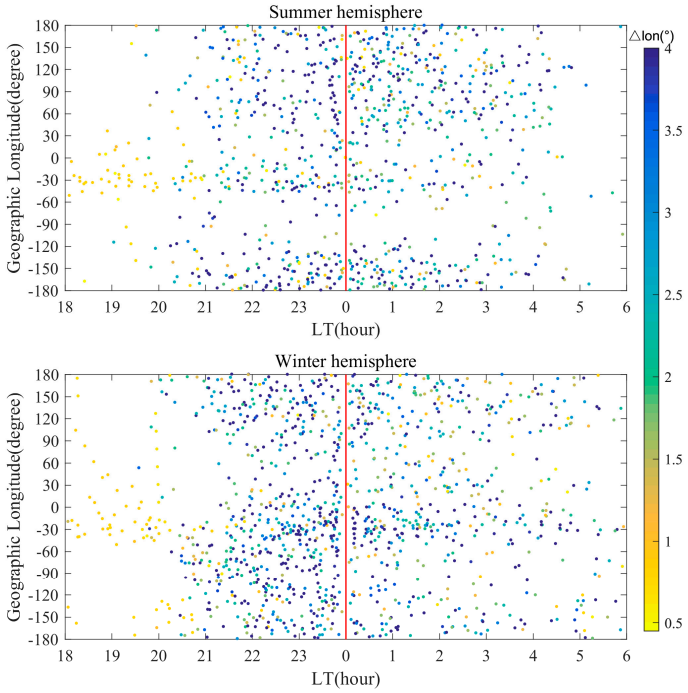

Figure 5. Longitude–local time variations of plasma blobs in equatorial regions with different longitude ranges in the summer hemisphere (**top**) and winter hemisphere (**bottom**) during 2000–2003. The red lines represent midnight.

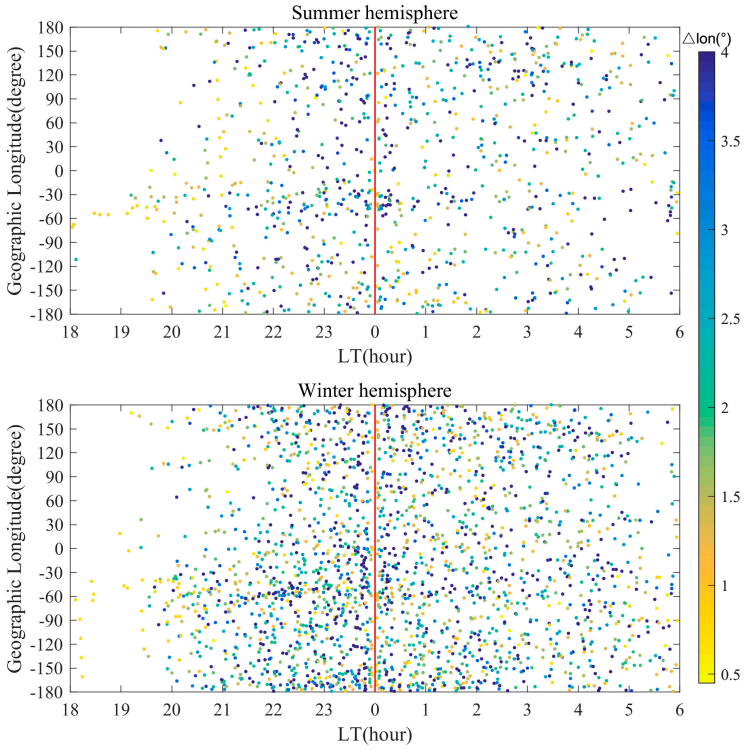

Figure 6. Same as Figure 5, but in low- to middle-latitude regions.

As shown in Figures 5 and 6, many more blobs occurred in the winter hemisphere in both equatorial and low- to middle-latitude regions. The distribution of plasma blobs shows the remarkable longitude and local time dependences in the equatorial and low- to middle-latitude regions. The peak occurrence of plasma blobs was around midnight, which is also consistent with previous studies [3,7,22].

4. Discussion

From some case studies, plasma bubbles and plasma blobs were recorded concurrently in close longitude regions; the occurrence of plasma blobs is linked with the evolution of plasma bubbles [8,23,24] due to a polarized electric field from EPBs. Plasma blobs also show some characteristics similar to those of EPBs, such as drift, temperature fluctuation, O^+ proportion and longitude range [7,23]. But the statistical characteristics of EPBs are very different from those of plasma blobs, as shown in Figures 2 and 3 and previous studies. Plasma blobs seem to be complementary to EPBs [2]. For instance, EPBs occur more frequently in equinoctial months, while blobs occur more in the two solstices, with a minimum in the two equinoxes. EPBs prefer to occur under high solar conditions, while blobs occur more frequently under the low solar flux level than under the high solar flux level [2]. The longitudinal distributions of EPBs and blobs also show differences. For example, the occurrence rate of EPBs in the 120~240°E sector is low [25], while the occurrence of blobs is high. In the 0~60°E sector, EPBs occur frequently, but the occurrence of blobs is not high. Bubbles often occur simultaneously in the conjugate hemispheres [26], while blobs usually occur only in one hemisphere (as shown in Figure 3), though blobs sometimes show the conjugated property [18]. Hence, EPBs would be not the major factor leading to the occurrence of blobs, though blobs may occur with the evolution of EPBs.

Due to some similarities in the occurrence climatology of blobs and MSTIDs [3,22], in addition to the observations of blobs at the locations of MSTIDs [14,27], the occurrence of blobs is proposed to link with MSTIDs. There are some different climatologies between blobs and MSTIDs. Though MSTIDs have the maximum occurrence in solstices, similar

to that of blobs, the annual and longitudinal distribution of MSTIDs shows a hemispheric symmetry and conjugacy [27,28]. The occurrence rate of MSTIDs is more frequent in the December solstice than in the June solstice in the European region [29], but more in the June solstice and more in the summer hemisphere [30]. Additionally, the longitudinal distribution of MSTIDs, which peaks in the 120~150°E region, is different from that of plasma blobs. Nighttime MSTIDs propagate equatorward [28], while field-aligned plasma flow within the blob is generally poleward with respect to the ambient [30]. Additionally, as described in linear growth rate of Perkins instability [7], it seems that the occurrence of plasma blobs is not related to Perkins instability, which is thought to be the major mechanism leading to the occurrence of nighttime MSTIDs [28].

Moreover, Su et al. [7] proposed that the nighttime Es layer, which is linked with the occurrence of MSTIDs, may be a candidate to lead to the formation of the blobs, due to the fact that the polarized electric field related to the Es layer can map to the F layer to cause F region density irregularities. The longitudinal morphology of the Es layer from CHAMP observations is similar to that of blobs in the June solstice, but the Es layer is preferable to occur in summer hemisphere [28,31].

Therefore, either plasma bubbles or MSTIDs are not necessary for the occurrence of plasma blobs; there would be other factors or mechanisms causing the formation of low-latitude plasma blobs. The seasonal and interhemispheric asymmetry of plasma blobs shown in Figures 3–6 would not be related to plasma bubbles or MSTIDs. Some studies also proposed that some blobs may be associated with EPBs; other blobs may be related to other factors [13,22].

Meridional wind is proposed to play an important role in the development and evolution of plasma blobs [9–11]. Thermospheric neutral winds have a direct effect on the transport of plasma in the ionosphere along magnetic field lines and on the generation of the electric field via wind dynamos. Indirectly, winds can modify the ionospheric composition via changes in the neutral composition [32].

In the northern and southern hemispheres, meridional winds inferred from Fabry–Perot interferometer (FPI) observations show variations with local time, season and longitude. In the magnetic northern hemisphere, at Arecibo (18.35°N, −66.75°E; geomagnetic lat: 27.1°N), the meridional wind is usually southward (equatorward) in summer (June solstice, May–August) and northward (poleward) in winter (December solstice, November–February) during 2000–0400 LT [33,34]. In the early evening of the March and September equinoxes, the meridional wind is northward and turns southward after 2100 LT [34].

In the magnetic southern hemisphere, at Arequipa (−16.5°N, −71.5°E; geomagnetic lat: −3.5°N), the nighttime (1800–0600 LT) meridional winds are predominately southward (poleward) in the June solstice (May–August) [32,33] and are northward (equatorward) during the November–February solstice. In the equinoctial months, meridional wind is southward around local sunset and turns northward around 2000 LT [33]. At Cajazeiras (−6.87°N, −38.56°E; geomagnetic lat: −5.73°N) and Cariri (−7.38°N, −36.52°E; geomagnetic lat: −6.81°N), in the summer months (December solstice), typical meridional wind is northward (equatorward), and the wind is southward (poleward) after sunset and lasts until the post-midnight in the winter months (June solstice), with peaks at around 2100 LT at ~50 m/s. The magnitude of meridional wind is slightly larger in the local summer months (November–February) than in the local winter months (May–August). During the equinoctial months, the meridional winds show two equatorward maxima (2300 LT and 0400 LT), and the magnitude is smaller than for the wind during the two solstices [35].

In Abuja, Nigeria (8.99°N, 7.39°E; geomagnetic lat: −1.60°N), meridional wind flowed southward (poleward) in March–June 2016 and northward (equatorward) in November–December 2017 and January 2018 around local sunset (1800–2000 LT). The magnitude of the

meridional winds is much stronger than has been reported in other longitudinal sectors; the maximum meridional wind is about 95 m/s [36].

The observational meridional winds in different longitudinal sectors all show a strong summer-to-winter transequatorial circulation in the solstices, which would inhibit the development of Rayleigh–Taylor instability and the occurrence of EPBs. This circulation helps to accumulate plasma in the winter hemisphere by ion-neutral collision. As revealed by Park et al. [30], field-aligned plasma flow within blob regions was generally poleward with respect to the background, and they proposed that the poleward flow seems to play an important role in generation or maintenance of blobs.

Thus, we can conclude that poleward meridional wind plays an important role in the occurrence of plasma blobs, resulting in seasonal and interhemispheric asymmetry of plasma blobs in the equatorial and low- to middle-latitude ionospheres. A question is, do low-latitude plasma blobs generate locally or originate from the equatorial region? If blobs generate locally in low-latitude regions, the effects of declination (D) and inclination (I) may not be ignored. Further, meridional wind in longitude dependence may be related to declination [37].

Thermospheric winds, with a meridional component Um (positive equatorward) and a zonal component Uz (positive westward), can induce F region plasma drift along the field line $V_{//}$ (positive upward), which can be approximated as $V_{//} = (Um\cos D + Uz\sin D)\cos I\sin I$ [38]. Therefore, equatorward (poleward) meridional winds result in positive (negative) $V_{//}$ transporting plasma upward (downward) into higher (lower) altitudes with slower (faster) chemical loss rates. Meridional winds are typically important in contributing to $V_{//}$ as declination is small, which is described by $Um\cos D\cos I\sin I$. As Um is poleward, D is large and I is small, and the drift is downward in the northern hemisphere and upward in the southern hemisphere, with a small value. The plasma can accumulate at a high altitude and reach equilibrium due to low recombination and ion-neutral collision, leading to the formation of density enhancement, which is consistent with the fact that the height of blobs is higher than the height of bubbles [3,8]. In contrast, D is small and I is large, and the drift is large; the plasma would move to a relative lower altitude and get a new balance due to the recombination and collision.

Assuming that the blobs generate locally in equatorial and low-latitude regions, in Figure 7, we display the longitudinal variations of inclination (I) and declination (D) at the equator, represented by solid lines, and their absolute values, represented by dashed lines.

From Figures 2–7, we can notice that as declination is large and inclination is small, the occurrence of blobs is high, such as in the −180~−120°E, −60~−30°E and 150~180°E sectors (the shaded yellow regions). And as declination is small and inclination is large, the occurrence is low, such as in the 90~120°E and −120~−90°E sectors (the shaded orange regions).

Furthermore, Figure 8 and Figure 9 present the distribution of plasma blobs with local time and dip latitude in the June solstice (May–August, a) and December solstice (November–February, b) during 2000–2003 in the 0–30°E and 300–330°E regions, respectively. The green circles represent the location of Abuja and Cariri, and the red arrows represent the direction of meridional wind. The dashed red lines represent the dip equator, and the dashed grey lines represent midnight.

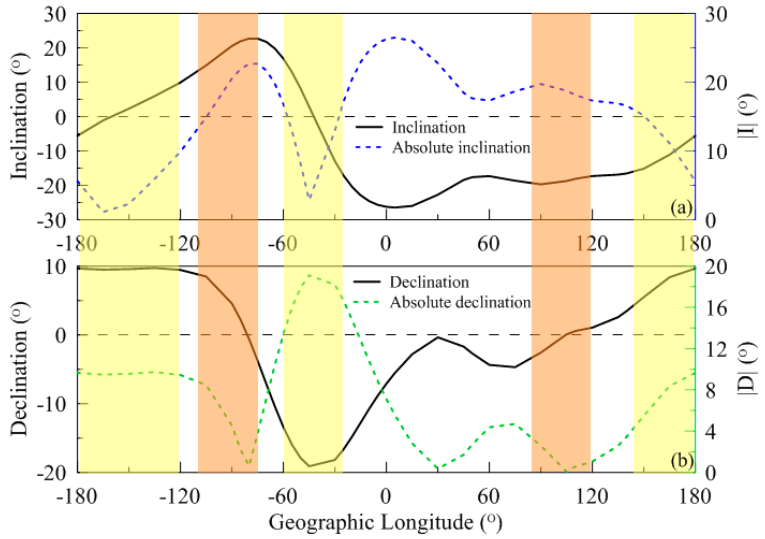

Figure 7. Longitudinal variations of inclination (I) and absolute value of inclination ($|I|$), declination (D) and absolute value of declination ($|D|$). The dashed blue and green lines represent the absolute values of inclination and declination, respectively.

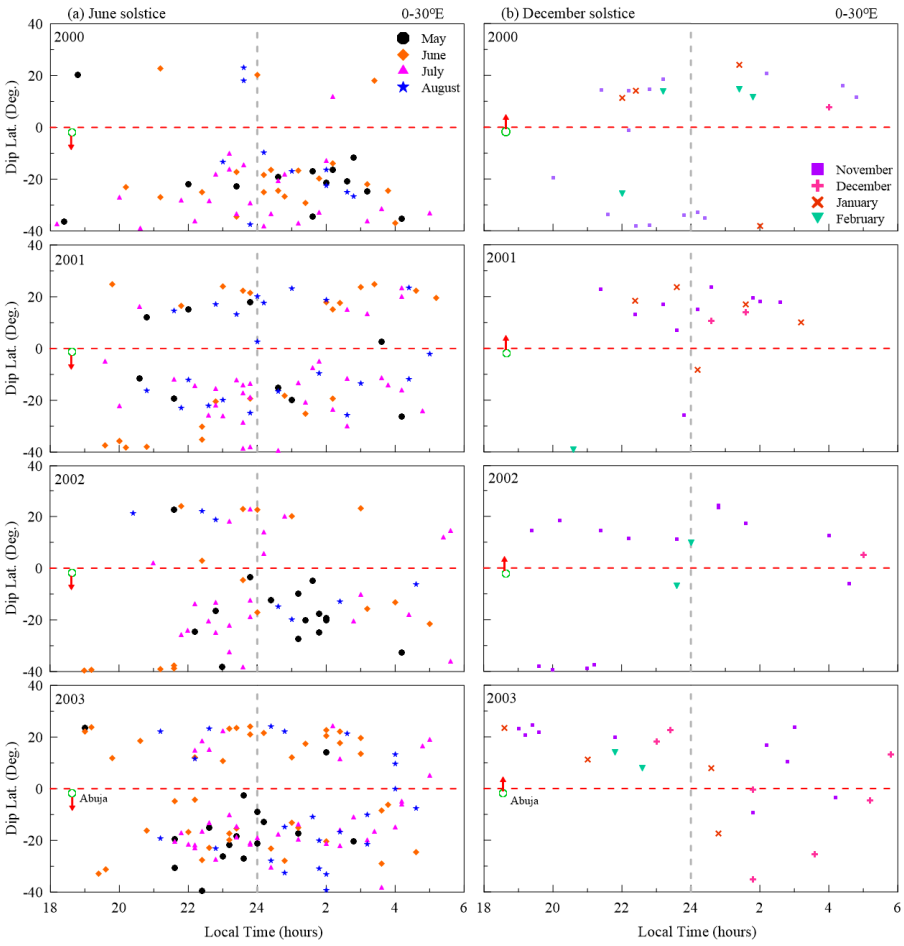

Figure 8. The distribution of plasma blobs with local time and dip latitude in the June solstice (May–August) and December solstice (November–February) during 2000–2003 in the 0–30°E region. The green circles represent the location of Abuja, and the red arrows represent the meridional wind. The dashed grey lines represent local midnight.

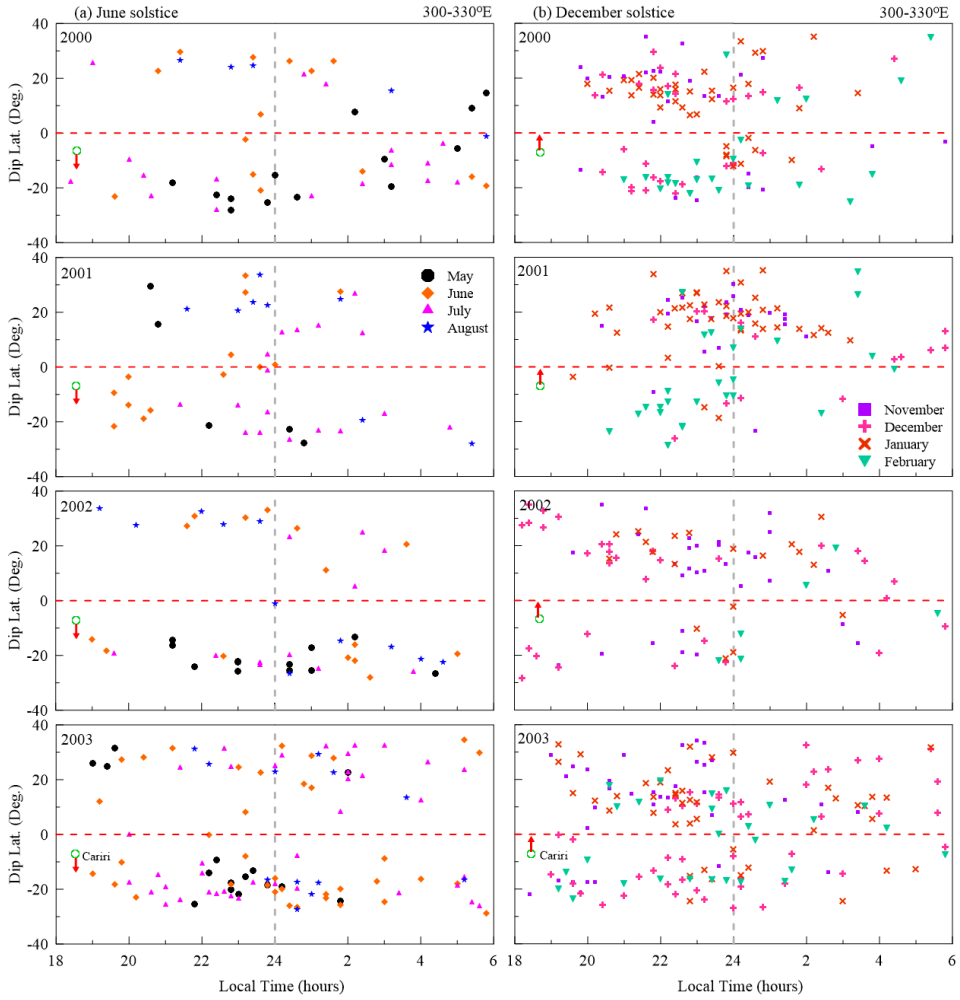

Figure 9. Same as Figure 8, but in the 300–330°E region. The green circles represent the location of Cariri, and the red arrows represent the meridional wind. The green circles represent the location of Cariri.

As shown in Figures 8 and 9, plasma blobs occurred mainly in the June solstice in the 0–30°E region and in the December solstice in the 300–330°E region. More blobs occurred in the hemisphere where the transequatorial meridional wind flows to. In the 0–30°E region (e.g., Abuja), in the June solstice, the transequatorial meridional wind flowed from the northern hemisphere (summer) to the southern hemisphere (winter), and more blobs occurred in the winter hemisphere. In the 300–330°E region (e.g., Cariri), in the December solstice, the transequatorial meridional wind flowed from the southern hemisphere (summer) to the northern hemisphere (winter), and more blobs also occurred in the winter hemisphere.

Moreover, the absolute value of declination is large and inclination is small in the 300–330°E region, while the absolute value of declination is small and inclination is large in the 0–30°E region; hence, plasma blobs occurred in the 300–330°E region (shown in Figure 9) much more than in the 0–30°E region (shown in Figure 8).

In addition, the distribution of plasma blobs also showed differences with different solar activities (year), as shown in Figures 8 and 9. It seems that the occurrence of plasma blobs would be higher with low solar activity. For instance, in the 0–30°E sector, in the northern hemisphere, the occurrence of blobs with lower solar activity (2003) was more remarkable than that with higher solar activity (2000) during the June solstice. In the

300–330°E sector, the blobs in 2003 were more than in 2000 during the June solstice, and the blobs in 2003 were more than in 2001–2002 during the December solstice.

There is still a question, as suggested by Figures 8 and 9: in some longitude regions, why do the blobs occur in some months (e.g., the June solstice) but not in other months (e.g., the December solstice)? This also indicates that there would be other factors for initiating the occurrence of plasma blobs. In conclusion, the longitudinal variation of plasma blobs would be related to declination and inclination, with the effect of meridional wind. In the end, another question about the effect of meridional neutral wind should be noted, whether would the wind be related to plasma instability, such as Perkins instability or E×B instability [39], affecting the initiation and evolution of plasma irregularities. Moreover, there would be other factors leading to the occurrence of plasma blobs; the effects of meridional wind and other factors on the formation and evolution of plasma blobs need still to be further studied, based on case studies and multiple observations.

5. Conclusions

Using the ROCSAT-1 observations during high solar activity (2000–2003), we studied the statistically climatology of plasma blobs in the low-latitude ionosphere. Distributions of plasma blobs display remarkable seasonal and interhemispheric asymmetry, with a higher occurrence in the winter months and in the winter hemisphere. The longitudinal and hemispheric distributions of plasma blobs are very different from those of EPBs or MSTIDs; either EPBs or MSTIDs are not necessary for the occurrence of plasma blobs. Based on the characteristics of meridional winds at different longitudes, we conclude that meridional wind (poleward) plays an important role in the occurrence of low-latitude plasma blobs, contributing to the seasonal and interhemispheric asymmetry of plasma blobs in the low-latitude ionosphere. Declination and inclination may control the longitudinal variation of plasma blobs, with the effect of meridional wind. There may be other key factors leading to the formation of plasma blobs, which need to be further studied from case and statistical studies. The characteristics of plasma blobs during low and medium solar activities also should be verified using long-term observations.

Author Contributions: Conceptualization, Z.H. and W.L.; methodology, J.Z. and W.L.; software, J.Z.; validation, Z.H., G.J. and Z.Z.; formal analysis, Z.Z. and S.C.; investigation, W.L.; resources, W.L. and Z.Z.; data curation, W.L.; writing—original draft preparation, Z.H and J.Z.; writing—review and editing, W.L. and S.C.; visualization, J.Z.; supervision, W.L.; project administration, W.L.; funding acquisition, W.L. All authors have read and agreed to the published version of the manuscript.

Funding: This research was funded by the Fundamental Research Funds for the Central Universities, South-Central MinZu University (Grant Number: CZZ24007).

Data Availability Statement: The ROCSAT-1 data can be downloaded from Coordinated Data Analysis Web (https://cdaweb.gsfc.nasa.gov/pub/data/formosat-rocsat/formosat-1/ipei/ (accessed on 1 June 2022)).

Acknowledgments: We acknowledge the use of ROCSAT-1 data from National Central University.

Conflicts of Interest: The authors declare no conflicts of interest.

References

1. Kelly, M.C. *The Earth's Ionosphere: Plasma Physics & Electrodynamics*, 2nd ed.; Academic: San Diego, CA, USA, 2009; ISBN 978-0-12-088425-4.
2. Watanbe, S.; Oya, H. Occurrence characteristics of low latitude ionosphere irregularities observed by impedance probe on board the Hinotori satellite. *J. Geomagn. Geoelectr.* **1986**, *38*, 125–149. [CrossRef]
3. Choi, H.S.; Kil, H.; Kwak, Y.S.; Park, Y.D.; Cho, K.S. Comparison of the bubble and blob distribution during the solar minimum. *J. Geophys. Res. Space Phys.* **2012**, *117*, A04314. [CrossRef]

4. Oya, H.; Takahashi, T.; Watanabe, S. Observation of low latitude ionosphere by the impedance probe on board the Hinotori satellite. *J. Geomagn. Geoelectr.* **1986**, *38*, 111–123. [CrossRef]
5. Park, J.; Min, K.W.; Kim, V.P.; Kil, H.; Kim, H.J.; Lee, J.J.; Lee, E.; Kim, S.J.; Lee, D.Y.; Hairston, M. Statistical description of low-latitude plasma blobs as observed by DMSP F15 and KOMPSAT-1. *Adv. Space Res.* **2008**, *41*, 650–654. [CrossRef]
6. Park, J.; Stolle, C.; Lühr, H.; Rother, M.; Su, S.Y.; Min, K.W.; Lee, J.J. Magnetic signatures and conjugate features of low-latitude plasma blobs as observed by the CHAMP satellite. *J. Geophys. Res. Space Phys.* **2008**, *113*, A09313. [CrossRef]
7. Su, S.Y.; Shih, Y.J.; Chao, C.K.; Tsai, L.C.; Liu, C.H. A statistical study on the occurrence characteristics of low-to-midlatitude ionospheric density enhancements (plasma blobs). *Adv. Space Res.* **2022**, *69*, 2957–2968. [CrossRef]
8. Le, G.; Huang, C.S.; Pfaff, R.F.; Su, S.Y.; Yeh, H.C.; Heelis, R.A.; Rich, F.J.; Hairston, M.R. Plasma density enhancements associated with equatorial spread F: ROCSAT-1 and DMSP observations. *J. Geophys. Res. Space Phys.* **2003**, *108*, A8. [CrossRef]
9. Huang, C.S.; Le, G.; de La Beaujardiere, P.A.; Roddy, P.A.; Hunton, D.E.; Pfaff, R.F.; Hairston, M.R. Relationship between plasma bubbles and density enhancements: Observations and interpretation. *J. Geophys. Res. Space Phys.* **2014**, *119*, 1325–1336. [CrossRef]
10. Krall, J.; Huba, J.D.; Martinis, C.R. Three-dimensional modeling of equatorial spread F airglow enhancements. *Geophys. Res. Lett.* **2009**, *36*, L10103. [CrossRef]
11. Krall, J.; Huba, J.D.; Joyce, G.; Yokoyama, T. Density enhancements associated with equatorial spread F. *Ann. Geophys.* **2010**, *28*, 327–337. [CrossRef]
12. Luo, W.H.; Xiong, C.; Zhu, Z.P.; Mei, X.F. Onset condition of plasma density enhancements: A case study for the effects of meridional wind during 17–18 August 2003. *J. Geophys. Res. Space Phys.* **2018**, *123*, 6714–6726. [CrossRef]
13. Park, J.; Huang, C.S.; Eastes, R.W.; Coster, A.J. Temporal evolution of low-latitude plasma blobs identified from multiple measurements: ICON, GOLD, and Madrigal TEC. *J. Geophys. Res. Space Phys.* **2022**, *127*, e2021JA029992. [CrossRef] [PubMed]
14. Park, J.; Martinis, C.; Lühr, H.; Pfaff, R.F.; Kwak, Y.S. Hemispheric asymmetry in transition from equatorial plasma bubble to blob as deduced from 630.0 nm airglow observations at low latitudes. *J. Geophys. Res. Space Phys.* **2016**, *121*, 881–893. [CrossRef]
15. Miller, E.S.; Kil, H.; Makela, J.J.; Heelis, R.A.; Talaat, E.R.; Gross, A. Topside signature of medium-scale traveling ionospheric disturbances. *Ann. Geophys.* **2014**, *32*, 959–965. [CrossRef]
16. Pimenta, A.A.; Sahai, Y.; Bittencourt, J.A.; Rich, F.J. Ionospheric plasma blobs observed by OI 630 nm all-sky imaging in the Brazilian tropical sector during the major geomagnetic storm of April 6–7, 2000. *Geophys. Res. Lett.* **2007**, *34*, L02820. [CrossRef]
17. Kil, H.; Choi, H.S.; Heelis, R.A.; Paxton, L.J.; Coley, W.R.; Miller, E.S. Onset conditions of bubbles and blobs: A case study on 2 March 2009. *Geophys. Res. Lett.* **2011**, *38*, L06101. [CrossRef]
18. Kil, H.; Kwak, Y.S.; Lee, W.K.; Miller, E.S.; Oh, S.J.; Choi, H.S. The causal relationship between plasma bubbles and blobs in the low-latitude F region during a solar minimum. *J. Geophys. Res. Space Phys.* **2015**, *120*, 3961–3969. [CrossRef]
19. Kil, H.; Paxton, L.J.; Jee, G.; Nikoukar, R. Plasma blobs associated with medium-scale traveling ionospheric disturbances. *Geophys. Res. Lett.* **2019**, *46*, 3675–3681. [CrossRef]
20. Su, S.Y.; Liu, C.H.; Ho, H.H. Distribution characteristics of topside ionospheric density irregularities: Equatorial versus midlatitude regions. *J. Geophys. Res. Space Phys.* **2006**, *111*, A06305. [CrossRef]
21. Smith, J.; Heelis, R.A. Equatorial plasma bubbles: Variations of occurrence and spatial scale in local time, longitude, season, and solar activity. *J. Geophys. Res. Space Phys.* **2017**, *122*, 5743–5755. [CrossRef]
22. Huba, J.D. Resolution of the equatorial spread F problem: Revisited. *Front. Astron. Space Sci.* **2023**, *9*, 1098083. [CrossRef]
23. Haaser, R.A.; Earle, G.D.; Heelis, R.A.; Klenzing, J.; Stoneback, R.; Coley, W.R.; Burrell, A.G. Characteristics of low-latitude ionospheric depletions and enhancements during solar minimum. *J. Geophys. Res. Space Phys.* **2012**, *117*, A10305. [CrossRef]
24. Yokoyama, T.; Su, S.Y.; Fukao, S. Plasma blobs and irregularities concurrently observed by ROCSAT-1 and equatorial atmosphere radar. *J. Geophys. Res. Space Phys.* **2007**, *112*, A05311. [CrossRef]
25. Su, S.Y.; Chao, C.K.; Liu, C.H. On monthly, seasonal/longitudinal variations of equatorial irregularity occurrences and their relationship with the postsunset vertical drift velocities. *J. Geophys. Res. Space Phys.* **2008**, *113*, A05307. [CrossRef]
26. Shiokawa, K.; Otsuka, Y.; Ogawa, T.; Wilkinson, P. Time evolution of high-altitude plasma bubbles imaged at geomagnetic conjugate points. *Ann. Geophys.* **2004**, *22*, 3137–3143. [CrossRef]
27. Kil, H.; Paxton, L.J. Global distribution of nighttime medium-scale traveling ionospheric disturbances seen by Swarm satellite. *Geophys. Res. Lett.* **2017**, *44*, 9176–9182. [CrossRef]
28. Otsuka, Y. Medium-scale traveling ionospheric disturbances. In *Space Physics and Aeronomy Collection: Ionosphere Dynamics and Applications*; Geophysical Monograph Series; American Geophysical Union: Washington, DC, USA, 2021; Volume 260. [CrossRef]
29. Otsuka, Y.; Suzuki, K.; Nakagawa, S.; Nishioka, M.; Shiokawa, K.; Tsugawa, T. GPS observations of medium-scale traveling ionospheric disturbances over Europe. *Ann. Geophys.* **2013**, *31*, 163–172. [CrossRef]
30. Park, J.; Lühr, H.; Stolle, C.; Rother, M.; Min, K.W.; Chung, J.K.; Kim, Y.H.; Michaelis, I.; Noja, M. Magnetic signatures of medium-scale traveling ionospheric disturbances as observed by CHAMP. *J. Geophys. Res. Space Phys.* **2009**, *114*, A03307. [CrossRef]

31. Wu, D.L.; Ao, C.O.; Haji, G.A.; Juarez, M.T.; Mannucci, A.J. Sporadic E morphology from GPS-CHAMP radio occultation. *J. Geophys. Res. Space Phys.* **2005**, *110*, A01306. [CrossRef]
32. Emmert, J.T.; Faivre, M.L.; Hernandez, G.; Jarvis, M.J.; Meriwether, J.W.; Niciejewski, R.J.; Sipler, D.P.; Tepley, C.A. Climatologies of nighttime upper thermospheric winds measured by ground-based Fabry-Perot interferometers during geomagnetically quiet conditions: 1. Local time, latitudinal, seasonal, and solar cycle dependence. *J. Geophys. Res. Space Phys.* **2006**, *111*, A12302. [CrossRef]
33. Biondi, M.A.; Sazykin, S.Y.; Fejer, B.G.; Meriwether, J.W.; Fesen, C.G. Equatorial and low latitude thermospheric winds: Measured quiet time variations with season and solar flux from 1980 to 1990. *J. Geophys. Res. Space Phys.* **1999**, *104*, 17091–17106. [CrossRef]
34. Brum, C.G.M.; Tepley, C.A.; Fentzke, J.T.; Robles, E.; Santos, P.T.; Gonzalez, S.A. Long-term changes in the thermospheric neutral winds over Arecibo: Climatology based on over three decades of Fabry-Perot observations. *J. Geophys. Res. Space Phys.* **2012**, *117*, A00H14. [CrossRef]
35. Fisher, D.J.; Makela, J.J.; Meriwether, J.W.; Buriti, R.A.; Benkhaldouun, Z.; Kaab, M.; Lagheryeb, A. Climatologies of nighttime thermospheric winds and temperatures from Fabry-Perot interferometer measurements: From solar minimum to solar maximum. *J. Geophys. Res. Space Phys.* **2015**, *120*, 6679–6693. [CrossRef]
36. Rabiu, A.B.; Okoh, D.I.; Wu, Q.; Bolaji, O.S.; Abdulrahim, R.B.; Dare-Idowu, O.E.; Obafaye, A.A. Investigation of the variability of night-time equatorial thermospheric winds over Nigeria, West Africa. *J. Geophys. Res. Space Phys.* **2021**, *126*, e2020JA028528. [CrossRef]
37. Luan, X.; Solomon, S.C. Meridional winds derived from COSMIC radio occultation measurements. *J. Geophys. Res. Space Phys.* **2008**, *113*, A08302. [CrossRef]
38. Zhang, S.R. Ionosphere and thermosphere coupling at mid- and subauroral latitudes. In *Space Physics and Aeronomy Collection: Ionosphere Dynamics and Applications*; Geophysical Monograph Series; American Geophysical Union: Washington, DC, USA, 2021; Volume 260. [CrossRef]
39. Maruyama, T. E×B instability in the F-region at low- to mid-latitudes. *Planet. Space Sci.* **1990**, *38*, 273–285. [CrossRef]